THE JOURNAL OF PHYSICAL CHEMISTRY B

Article

pubs.acs.org/JPCB

Kinetic and Thermodynamic Fragilities of Square Well Fluids with Tunable Barriers to Bond Breaking

Anshul D. S. Parmar[†,‡] and Srikanth Sastry*[,†]

[†]Jawaharlal Nehru Centre for Advanced Scientific Research, Bengaluru 560 064, India

[‡]TIFR Centre for Interdisciplinary Sciences, Hyderabad 500 075, India

ABSTRACT: An understanding of the origin of *fragility*, which the rapidity of change of viscosity and related dynamical quantities, has been sought by a variety of approaches over the years. Within the framework of the Adam−Gibbs relation, fragility is in principle related to both the temperature variation of configurational entropy and the high temperature activation energy. Many theoretical analyses have been focused on the variation of configuration entropy, although the importance of the high temperature activation energy in determining the fragility of a glass former has also been emphasized. We explore the latter aspect by considering a model liquid whose high temperature activation energy is modified *by hand*, through the introduction of a tunable barrier to bond breaking. We show that changes in such a barrier are able to modify the fragility measured from the temperature dependence of dynamical quantities, while a thermodynamic measure of fragility obtained from the configurational entropy remains unchanged. We discuss the implications of our results to our understanding of fragility, and outline open questions that merit further investigation.

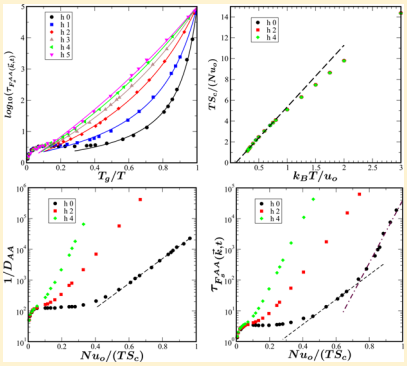

INTRODUCTION

The rapid rise of viscosity and relaxation times in supercooled liquids, leading to the glass transition, at which viscous liquids transform to an amorphous solid state, is a subject of long-standing investigation. Apart from the nature of the glass state, and the glass transition, understanding the strong, super-Arrhenius, temperature dependence of the viscosity and relaxation times, and rationalizing the observed diversity in manner in which the large viscosities at the glass transition are attained, have attracted considerable attention. How quickly viscosity and relaxation times increase as one cools a glass forming liquid is quantified by *fragility*.[1] Quantification of fragility amounts to characterizing the degree of super-Arrhenius behavior, which is material specific and has proved to be useful in organizing and understanding the diversity of behavior seen in glass formers.[2] Fragility is easily visualized, e.g., through the celebrated Angell plot[1] of the logarithm of the viscosity vs the inverse temperature scaled by the glass transition temperature T_g. Fragile liquids display deviation from Arrhenius behavior, the degree of deviation being an indication of the degree of fragility, whereas strong liquids display nearly Arrhenius behavior. Many quantitative measures of the degree of deviation from Arrhenius behavior, or fragility, have been described in the literature. Two of the commonly used quantifications are in terms of the [i] steepness index (m) and [ii] Vogel−Fulcher−Tammann (VFT) fits to the temperature dependence of relaxation times or viscosity.

The steepness index m is defined to be the slope of the logarithm of viscosity at the glass transition temperature T_g, with respect to scaled inverse temperate T_g/T:

$$m = \left[\frac{\mathrm{d}(\log \tau)}{\mathrm{d}\left(\frac{T_g}{T}\right)}\right]_{T=T_g} \tag{1}$$

From VFT fits to dynamic quantities (viscosity, relaxation times, or the diffusion coefficient), one can quantify fragility K_{VFT} by employing the form (shown for relaxation times)

$$\tau(T) = \tau_o \exp\left[\frac{1}{K_{VFT}\left(\frac{T}{T_{VFT}} - 1\right)}\right] \tag{2}$$

which defines kinetic fragility (K_{VFT}) assuming that relaxation times diverge at the temperature T_{VFT}. We distinguish in what follows the steepness index m and K_{VFT} *kinetic* measures of fragility from *thermodynamic* fragility.

In order to define thermodynamic fragility, we employ the Adam−Gibbs relation,[3] that relates growing relaxation times to a decrease in the configurational entropy S_c:

$$\tau(T) = \tau_o \exp\left[\frac{A}{TS_c(T)}\right] \tag{3}$$

The Adam−Gibbs relation is based on a picture of cooperatively rearranging regions (CRRs) which lead to

Special Issue: Biman Bagchi Festschrift

Received: March 31, 2015
Revised: July 2, 2015
Published: July 2, 2015

DOI: 10.1021/acs.jpcb.5b03122
J. Phys. Chem. B 2015, 119, 11243−11252

relaxation, and whose size increases with a lowering of temperature. The coefficient A may be viewed as being related to the high temperature activation energy, by noting that a constant high temperature S_c, $S_{c\infty}$, would lead to an Arrhenius temperature dependence with activation energy $E_\infty = A/(S_{c\infty}/k_B)$. We refer to it in what follows as a high temperature activation free energy, since A has in principle both enthalpic and entropic contributions. The configurational entropy, S_c, associated with the multiplicity of structures in a liquid, is obtained by subtracting the "vibrational" contribution from the total entropy. In the simplest procedure, this is accomplished by subtracting the entropy of the crystal from the total liquid entropy. Such a procedure was employed by Martinez and Angell, who showed a correlation between kinetic and thermodynamic fragilities defined using the temperature variation of the excess entropy.[4] However, the excess entropy can also include a vibrational contribution, since the crystal and liquid (or glass) vibrational entropies are not identical, and the latter can vary with a temperature dependent change in structure. The relevance of this has also been discussed in ref 4 with particular reference to constant pressure conditions, in ref 8, and much earlier by Goldstein.[5] Such a limitation does not apply to an evaluation of configurational entropy by subtracting the vibrational contribution in the liquid state without reference to the crystal, as in the inherent structure approach.[8] In the inherent structure approach,[6] S_c is associated with the number of local energy minima or inherent structures, and has been computed in many computational studies (e.g., refs 7 and 8 and other work mentioned in refs 9 and 10). A number of studies[11−17] have addressed the manner in which the fragility of a glass former may be determined by its composition, the nature of the interparticle interactions, etc.

If the temperature dependence of S_c is given by

$$TS_c = K_T\left[\frac{T}{T_K} - 1\right] \tag{4}$$

the Adam−Gibbs relation yields the VFT relation with the identification $K_{VFT} = K_T/A$, $T_{VFT} = T_K$ and K_T is a thermodynamic measure of fragility. The thermodynamic fragility K_T can be understood in terms of parameters of the potential energy landscape, the distribution of inherent structures, and vibrational or basin entropy corresponding to inherent structures on these energies.[8] In addition to K_T, the activation free energy A can influence the kinetic fragility, as has been emphasized as a general consideration in the past,[18] and arises more specifically in the context of discussions of density−temperature scaling.[19−22] Some of this discussion was anticipated by Angell[23] who considered a "kinetic" contribution to the fragility that might arise from the presence of barriers to bond-breaking (though the application of this idea to hydrogen bonded liquids was inconclusive). A notable recently studied example of the role of the high temperature activation free energy A is the analysis of the fragilities of model liquids with differing softness of interaction.[17] It is found that, as the softness of the interactions is increased, the kinetic fragilities *increase*, while the thermodynamic fragilities *decrease*. A rationalization of these results requires consideration of the variation of A with the softness of interactions. Inclusion of the variation of A, which needs to be estimated from high temperature data, results in a satisfactory, but not highly quantitatively accurate, estimation of the variation of kinetic fragilities with the softness of interactions.

In view of the above discussion, further analysis of the role of the activation free energy A in determining fragility is desirable. An appealing avenue to do so is to study a model system wherein the high temperature activation energy can be tuned without affecting the thermodynamics of the system. In this paper, we study such a model liquid, for which the bond lifetime can be tuned.[24] This model has previously been studied in the context of dynamical arrest in short-range attractive colloids,[25,26] which exhibits a diffusivity maximum in the studied attraction and density range.

We begin in the next section with a description of the model and the methods employed to study it, followed by a presentation of results, a discussion of their implicaitons, and concluding remarks.

MODEL AND METHODS

Model. We study a 50:50 binary mixture with hard core repulsion between particles followed by an attractive square well, with a tunable barrier at its outer edge. The ratio of diameters of the two types of particles is 1.20, with $\sigma_{AA} = 1.20\sigma_{BB}$. Further, for the AB interaction, the hard core diameter is additive, with $\sigma_{AB} = (\sigma_{AA} + \sigma_{BB})/2$.

The interaction potential, illustrated in Figure 1, is given by

$$u_{ij}(r) = \begin{cases} \infty & r_{ij} < \sigma_{ij} \\ -u_o & \sigma_{ij} < r_{ij} < \sigma_{ij} + \Delta_{ij} \\ h & \sigma_{ij} + \Delta_{ij} < \sigma_{ij} + \Delta_{ij} + w^B \\ 0 & \text{otherwise} \end{cases}$$

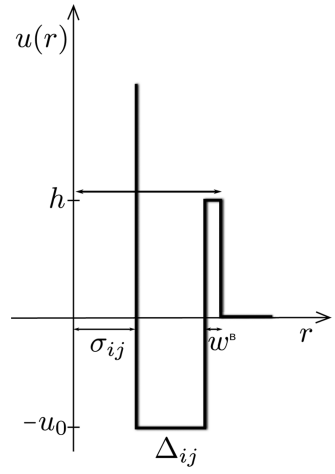

Figure 1. Schematic representation of the interaction potential. Here σ_{ij} is the hard sphere diameter, the attractive shell width is Δ_{ij}, and the width of the barrier of height h is w^B.

where r is the distance between particle i and j. The depth of the attractive shell is u_0, and the width Δ_{ij} of the square well is such that $\Delta_{ij}/(\sigma_{ij} + \Delta_{ij}) = 0.03$. Particles are considered to be bonded if they lie within the attractive shell (i.e., $\sigma_{ij} < r_{ij} < \sigma_{ij} + \Delta_{ij}$). The height h of the barrier is tunable and the width $w^B = 3 \times 10^{-4}\sigma_{BB}$. This thin and tunable barrier allows us to modulate the bond lifetime without affecting the thermodynamics of the system.[24]

We use reduced units throughout, with distances expressed in units of the smaller particle diameter σ_{BB}, energies (and temperatures) in the units of the square well depth u_o, and

DOI: 10.1021/acs.jpcb.5b03122
J. Phys. Chem. B 2015, 119, 11243−11252

time t in units of $\sigma_{BB}(m/u_o)^{1/2}$. The packing fraction is defined as $\phi = (\sum_i \rho_i \sigma_{ii}^3)(\pi/6)$, where $i \in [A, B]$, ρ_i is the number density, and σ_{ii} is the diameter of particle type i.

Since the particles interact via a pair potential that changes discretely, we perform event driven molecular dynamics simulations in a cubic box with periodic boundary conditions. All particles travel in straight line trajectories at constant velocity between successive collisions. Collision times between pairs of particles are calculated for relative separations where the potential changes discontinuously[27] and velocities are updated accordingly. Constant NVT simulations have been performed for $N = 256$ particles using the Lowe−Anderson thermostat[28,29] for the temperature range $T \in [0.28, 40.0]$ and barrier heights $h \in [0, 5]$ with run length $> 100\tau_\alpha$. (τ_α is the relaxation time, which will be described in the next section.)

Methods. Dynamics is characterized by the α relaxation times obtained by the self-intermediate scattering function, and the diffusion coefficient, from the mean squared displacements. The α relaxation time is calculated for particles of type A, as the time at which the self-intermediate scattering function $F_s^{AA}(\vec{k}, t)$ at $k = 2\pi$ decays to a value of $1/e$. $F_s^{AA}(\vec{k}, t)$ is calculated using

$$F_s^{AA}(\vec{k}, t) = \frac{1}{N_A}\left\langle \sum_{i=1}^{N_A} \exp(-i\vec{k}.(\vec{r}_i(t) - \vec{r}_i(0)))\right\rangle \tag{5}$$

where $\vec{r}_i(t)$ are the positions of particle i at time t and the averaging is done over all initial times.

Configurational Entropy. Configurational entropy is calculated by subtracting from the total entropy[30] of the system the vibrational component:

$$\mathcal{S}_c(T) = \mathcal{S}_{total}(T) - \mathcal{S}_{vib}(T) \tag{6}$$

The total entropy of the liquid is obtained via thermodynamic integration (TI)[31,32] from the ideal gas limit.[30] The pressures are estimated from collision rates[33] using

$$\frac{\beta P}{\rho} = 1 + \frac{\beta}{3N\mathcal{T}} \sum_{\text{events}} [\vec{r}_{jk}.\delta\vec{p}]_{\text{event}} \tag{7}$$

where $\mathcal{T}$ is the total time of the simulation and the summation is over collisions that occur between all pairs of particles j and k. The pressure is integrated over densities at a high reference temperature of $k_B T_{ref}/u_o = 50$, and further potential energies were integrated with respect to temperature at the desired packing fraction of $\phi = 0.55$ to evaluate the total entropy at any desired temperature.

In the inherent structure formalism,[6] the configuration space is partitioned into basins of attraction of local minima of the PEL, known as inherent structures (IS) and the vibrational free energy and entropy evaluated by a partition function integral over a basin.[9] However, for the system with the discrete interaction potential that we consider, it has been proposed that the basins can be identified with a given bond pattern,[34] a procedure which avoids the necessity to make any approximations in order to evaluate the basin entropy. We follow the same procedure here, and evaluate the basin free energies from thermodynamic integration with respect to an Einstein crystal reference state. A perturbation $\mathcal{H}_\lambda(\vec{r}, \lambda) = \lambda \sum_{i=1}^N (\vec{r}_i - \vec{r}_i^{\,o})^2$ is added to the original interaction Hamiltonian $\mathcal{H}_o$, and Monte Carlo simulations are performed for a range of λ values, subject to the constraint that the bond pattern remains invariant during the simulation, up to a maximum λ_{max} at which the free energy is obtained using only the perturbation term. Excess free energy of the model can then be calculated from this reference system in the usual way, as

$$\mathcal{F}_{vib}^{ex}(T, \lambda = 0) = \mathcal{F}_{vib}^{ex}(T, \lambda_{max}) - \int_{-\infty}^{\ln \lambda_{max}} \lambda \left\langle \sum_{i=1}^{N} (\vec{r}_i - \vec{r}_i^{\,o})^2 \right\rangle_\lambda \mathrm{d}(\ln \lambda) \tag{8}$$

where $\vec{r}_i^{\,o}$ represents the reference configuration we start with. For λ_{max}, the system sees only the harmonic confining potential, and the condition $\lambda_{max} \sum_{i=1}^N (\vec{r}_i - \vec{r}_i^{\,o})^2 = 3Nk_BT/2$ obeyed. On the basis of this, the basin entropy can be written as

$$\frac{\mathcal{S}_{vib}^{ex}}{Nk_B} = \frac{3}{2}\ln\left(\frac{\pi k_B T}{\lambda_{max}}\right) - 1 + \ln\left(\frac{N}{V}\right) + x_A \ln x_A + x_B \ln x_B + \beta \int_{-\infty}^{\ln \lambda_{max}} \lambda \left\langle \sum_{i=1}^{N} (\vec{r}_i - \vec{r}_i^{\,o})^2 \right\rangle_\lambda \mathrm{d}(\ln \lambda) \tag{9}$$

where x_i, $i \in [A, B]$, is the fraction of each type of particle. Equation 9 is the exact expression for the basin entropy $\mathcal{S}_{vib}^{ex}$ for the model. In Figure 2, we show the calculated λ dependence of $\beta\lambda\langle\sum_{i=1}^N (\vec{r}_i - \vec{r}_i^{\,o})^2\rangle_\lambda/N$ for various temperatures. At sufficiently large values of harmonic perturbation ($\lambda_{max} \approx 10^{10}$), the particles are localized in a much narrower space compared to the attractive shell and the square well interactions are irrelevant.

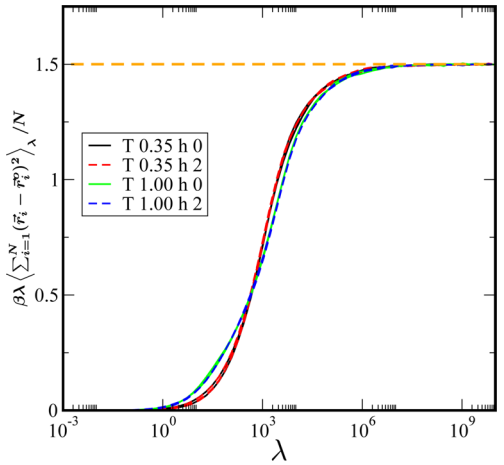

Figure 2. Thermodynamic integration scheme to estimate the basin entropy. λ dependence of $\beta\lambda\langle\sum_{i=1}^N (\vec{r}_i - \vec{r}_i^{\,o})^2\rangle_\lambda/N$ for different temperatures and barrier values. Clearly, the barrier heights do not affect the value of the quantity shown. The horizontal line indicates the expected value 3/2 for the purely harmonic behavior.

RESULTS

Dynamics. In Figure 3, we show the self-intermediate scattering function $F_s^{AA}(k, t)$ for $k\sigma_{BB} = 2\pi$ and the mean squared displacement for a range of temperatures. The data show that the dynamics gets slower as the temperature decreases. Next, we show in Figure 4 these quantities for a fixed temperature of $T = 0.8$ for various values of barrier height h. Clearly, the increasing of the barrier height has the expected effect of slowing down the dynamics. We expect that the *cage size* at which transient localization occurs for finite barriers to bond breaking will be dictated by the width of the attractive well rather than the location of the neighbors, but further analysis is required to validate this expectation.

DOI: 10.1021/acs.jpcb.5b03122
J. Phys. Chem. B 2015, 119, 11243−11252

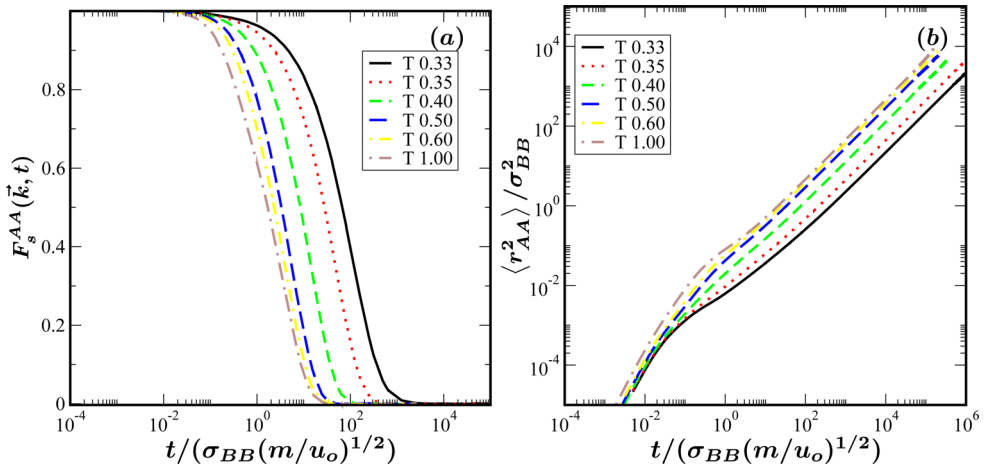

Figure 3. Dynamical properties for $h = 0$. (a) The self-intermediate scattering function at $k\sigma_{BB} = 2\pi$ displays longer relaxation times at lower temperatures. (b) The mean squared displacement (MSD) indicates a decrease in diffusion coefficient as temperature decreases.

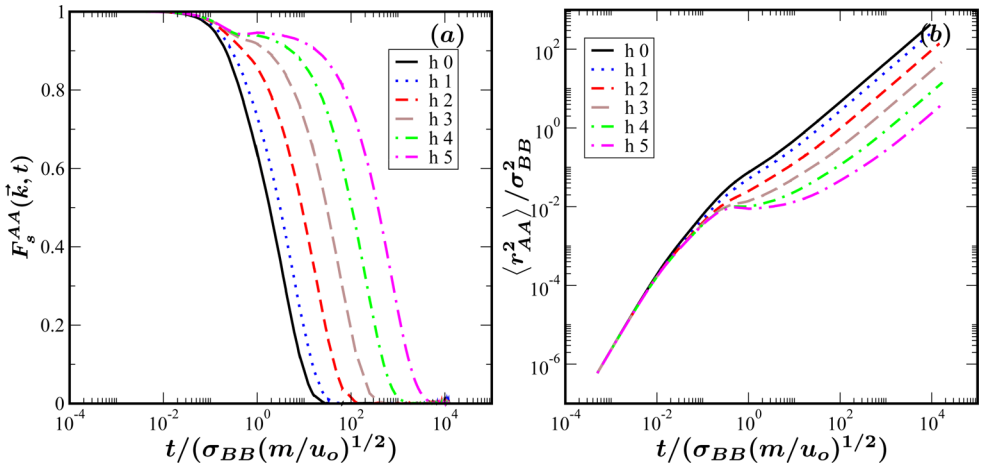

Figure 4. Dynamics slows down with increase in barrier height. (a) The self-intermediate scattering function and (b) mean squared displacement, at temperature $T = 0.80$, for different barrier heights h.

To study the variation of kinetic fragility with a change of barrier heights, we plot relaxation times τ obtained from the $F_s^{AA}(k, t)$ and the diffusion coefficients D_{AA}, in an "Angell" plot, where the temperature is scaled with a "glass transition" temperature, where the relaxation times reach a value of 10^5. From Figure 5, we see clearly that the apparent effect of a change in barrier height is to decrease the fragility of the liquid. We also note that the relaxation times and diffusion coefficients display a nonmonotonicity at high temperatures, which we return to later. Figure 5 also shows VFT fits to the data, both in the Angell plot and in linearized VFT form. From these fits, we obtain values of the kinetic fragility K_{VFT} and the Kauzmann temperature T_K which are listed in Tables 1 and 2, respectively, for relaxation times and diffusion coefficients. As noted, K_{VFT} decreases as h increases, as does T_K.

Thermodynamics. In order to assess thermodynamic aspects of the barriers, we consider here various static quantities for varying barrier heights. Since the barrier width is infinitesimal ($=3 \times 10^{-4}\sigma_{BB}$), we expect a negligible influence of the barrier height of static properties. The pair correlation functions, pressure, and average potential energy, shown in Figure 6, clearly demonstrate this to be the case.

From the pressure and potential energy data, we calculate the total excess entropy from thermodynamic integration as described earlier. Shown in Figure 7, the excess entropy too does not depend on the barrier heights h.

We next show in Figure 8 the basin entropies computed as described earlier from thermodynamic integration. The basin entropies too do not depend on the barrier heights h. Thus, we conclude that the introduction of a barrier to bond breaking, while influencing the dynamics strongly, has no bearing on the thermodynamics.

Relationship between Dynamic and Thermodynamic Quantities. Before discussing the temperature variation of the configurational entropy in the context of fragility, we discuss the high temperature behavior of S_c and diffusion coefficient D_{AA}. Shown in Figure 9, both of these quantities display the presence of a local maximum around $T = 0.8$. Such behavior has been observed for the square well and related models before[25,26] where attention was drawn to the fact that the variation of the configurational entropy captures the interesting nonmonotonicity of the diffusion coefficient.

Figure 10 shows $TS_c(T)$ as a function of T, and as would be expected in order to recover the VFT relation, $TS_c(T)$ exhibits linear behavior at low temperatures, which allows us to identify a Kauzmann temperature ($T_K = 0.11$) and a thermodynamic fragility ($K_T = 0.72$) from plotting $TS_c(T)$ vs T/T_K. Curiously,

DOI: 10.1021/acs.jpcb.5b03122
J. Phys. Chem. B 2015, 119, 11243−11252

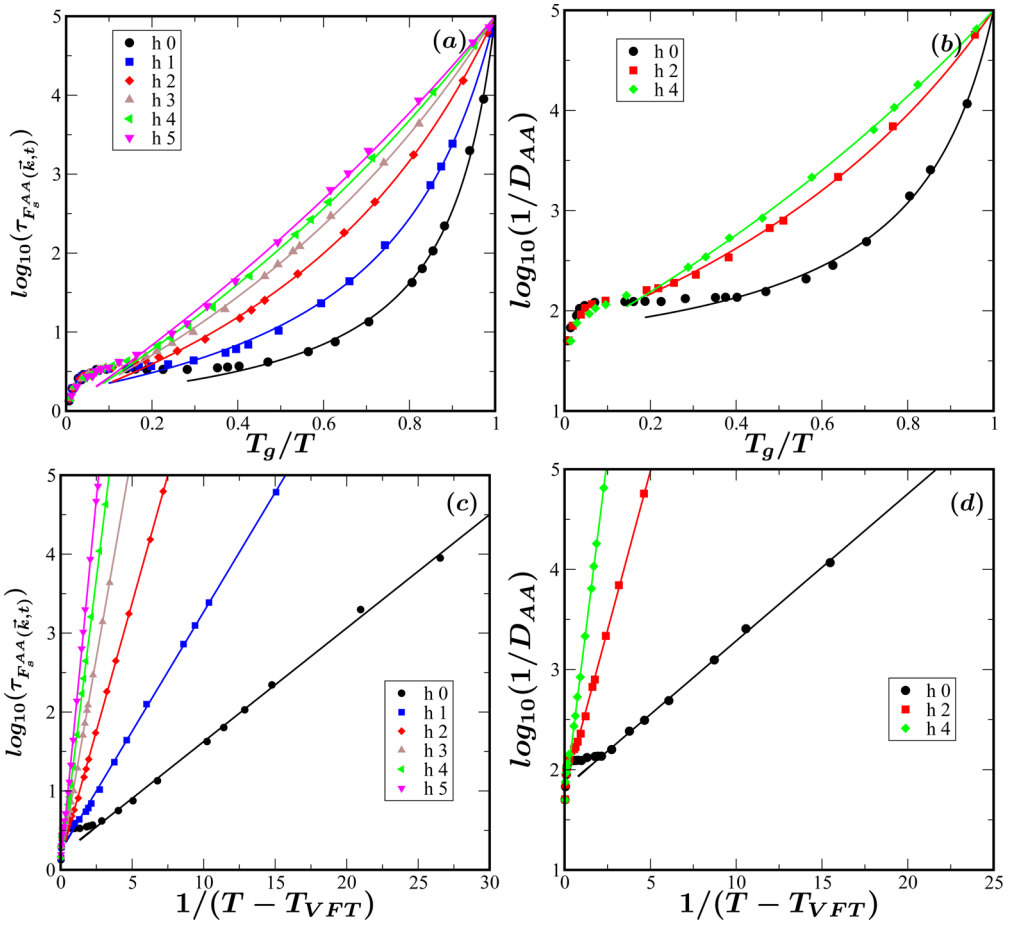

Figure 5. Kinetic fragility decreases with increase in barrier height. (a) Angell plot for relaxation times and (b) diffusion coefficients. The "glass transition" temperature T_g corresponds to a reference relaxation time of 10^5. The lines are VFT fits. (c) Relaxation times and (d) diffusion coefficients are shown in linearized VFT form.

Table 1. Comparison of the Kinetic Fragility and the Kauzmann Temperature for Various Barrier Heights Obtained from VFT Fits to Relaxation Times[a]

	barrier height					
parameters	$h = 0$	$h = 1$	$h = 2$	$h = 3$	$h = 4$	$h = 5$
K_{VFT}	0.762	0.335	0.128	0.066	0.040	0.027
T_K	0.252	0.234	0.191	0.159	0.134	0.117

[a]The table shows that fragility decreases with increasing barrier height.

Table 2. Comparison of the Kinetic Fragility and the Kauzmann Temperature for Various Barrier Heights Obtained from VFT Fits to the Diffusion Coefficients[a]

	barrier height		
parameters	$h = 0$	$h = 2$	$h = 4$
K_{VFT}	0.700	0.125	0.0514
T_K	0.235	0.184	0.1626

[a]The table shows that fragility decreases with increasing barrier height.

these values are not consistent with any of the kinetic fragility and VFT temperatures we find.

Next, we show in Figure 11 the plots of relaxation times and diffusion coefficients against TS_c in an Adam−Gibbs plot, for a range of barrier heights. We note that the data for different barrier heights clearly do not overlap, and further show a marked deviation from the Adam−Gibbs relation, eq 3. A substantial part of this deviation arises from the nonmonotonic or nearly nonmonotonic behavior observed at high temperatures. For relaxation times, however, even low temperature data for $h = 0$ do not show very good agreement with the Adam−Gibbs form, while, for diffusion coefficients, the behavior is in much closer conformity with the Adam−Gibbs relation. We return to the possible origins of this behavior shortly. However, the data in Figure 11 clearly shows that a change in barrier heights to bond breaking strongly affects the relationship between dynamical quantities and the configurational entropy.

However, since we know the exact origin of the differences in dynamics, we are in a position to seek simple relations between dynamics for different h values. A simple minded expectation, tested in Figure 12, is that the addition of the barrier modifies the "microscopic" time τ_o for relaxation processes, and by assuming that such modification is given by a Boltzmann factor to bond breaking, we may write

$$\tau_o = \tau_o^{(o)} \exp(h/k_B T) \tag{10}$$

where $\tau_o^{(o)}$ is the assumed constant prefactor for $h = 0$. Thus, the data for different h values should collapse when scaled by the factor $\exp(h/k_B T)$. As seen in Figure 12, this expectation is satisfied at low temperatures, but surprisingly, at high temperatures, it is not. The physics associated with the diffusivity maximum apparently is nontrivial and not simply scaled out.

DOI: 10.1021/acs.jpcb.5b03122
J. Phys. Chem. B 2015, 119, 11243−11252

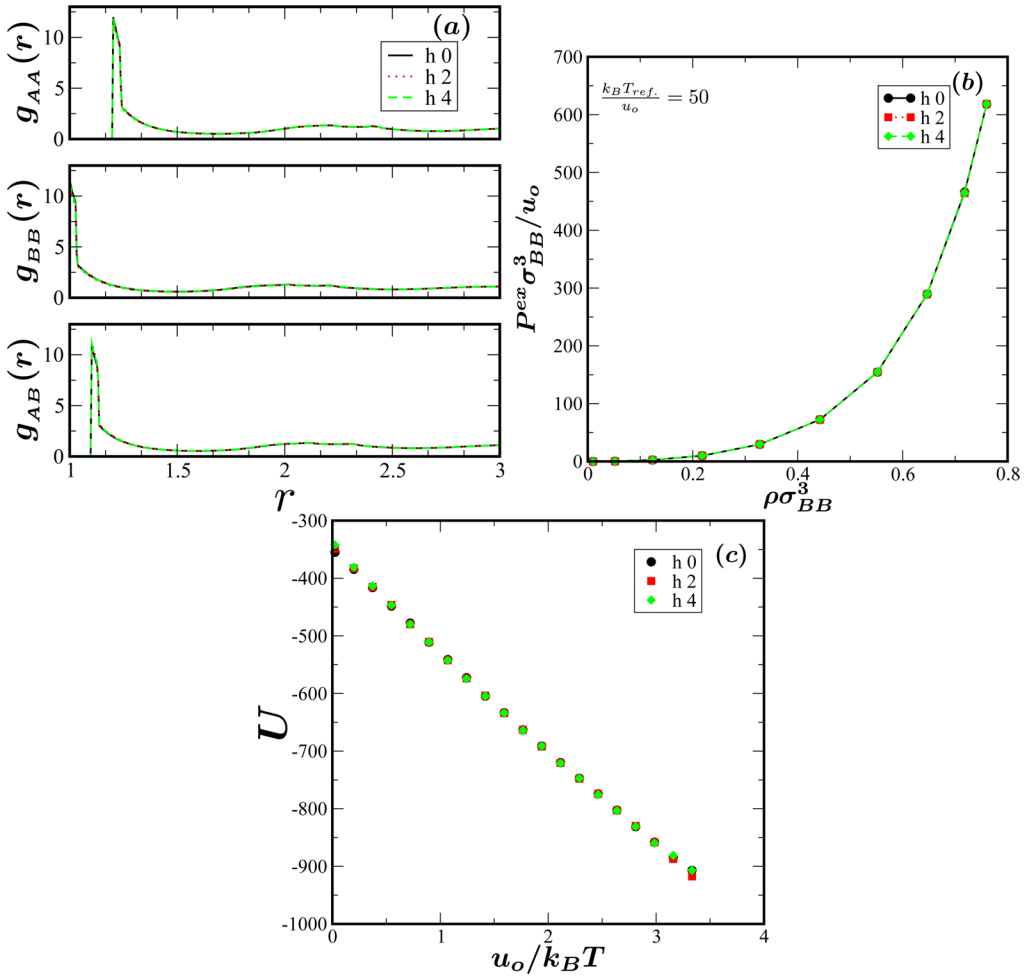

Figure 6. There is no effect significant of the barrier height on thermodynamic and structural quantities as seen by the invariance of (a) the radial pair correlation functions (shown for $T = 1.00$), (b) the excess pressure (vs density at reference temperature $T_{ref} = 50$), and (c) the average potential energy at packing fraction $\phi = 0.55$ over a wide temperature range.

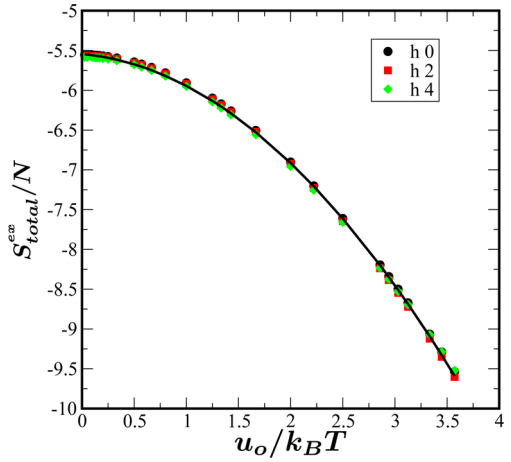

Figure 7. Temperature dependence of the total excess entropy for various barrier heights. Since the pressure and mean potential energies are the same regardless of barrier height, the estimated total excess entropy does not depend on the barrier height.

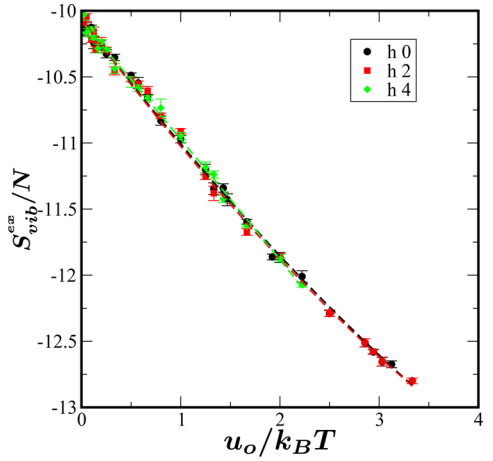

Figure 8. Temperature dependence of the basin entropy for various barrier heights, demonstrating that the basin entropy does not depend on the barrier height.

In order to understand the relation between dynamical data for different barrier heights in the context of the Adam−Gibbs relation, we write for $h = 0$

$$\ln \tau = \ln \tau_o + A/TS_c \quad (11)$$

For other values of h, we may write τ_o as $\tau_o = \tau_o^{(o)} \exp(h/k_BT)$. From this, we may write

$$\ln \tau = \ln \tau_o^{(o)} + A(h)/TS_c \quad (12)$$

DOI: 10.1021/acs.jpcb.5b03122
J. Phys. Chem. B 2015, 119, 11243−11252

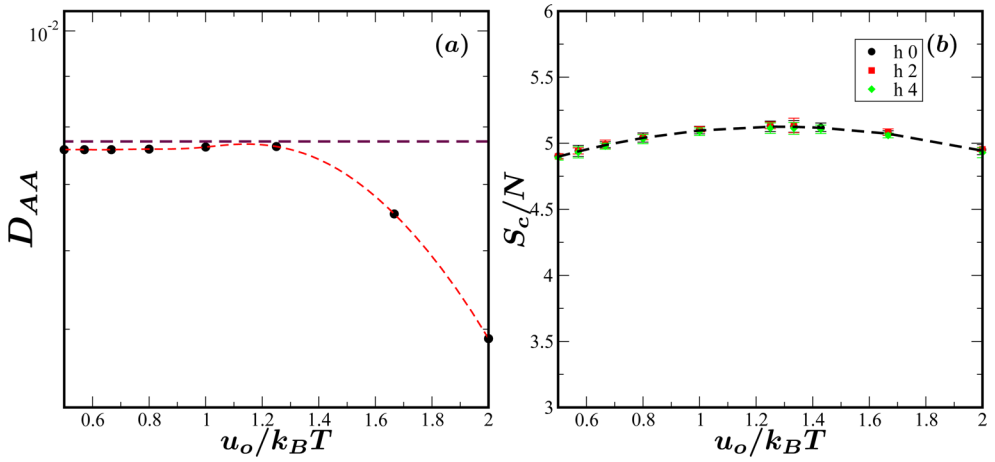

Figure 9. Diffusion coefficient exhibiting a shallow maximum in temperature for $h = 0$ at high temperature. The configurational entropy S_c also shows a corresponding maximum in the same temperature range.

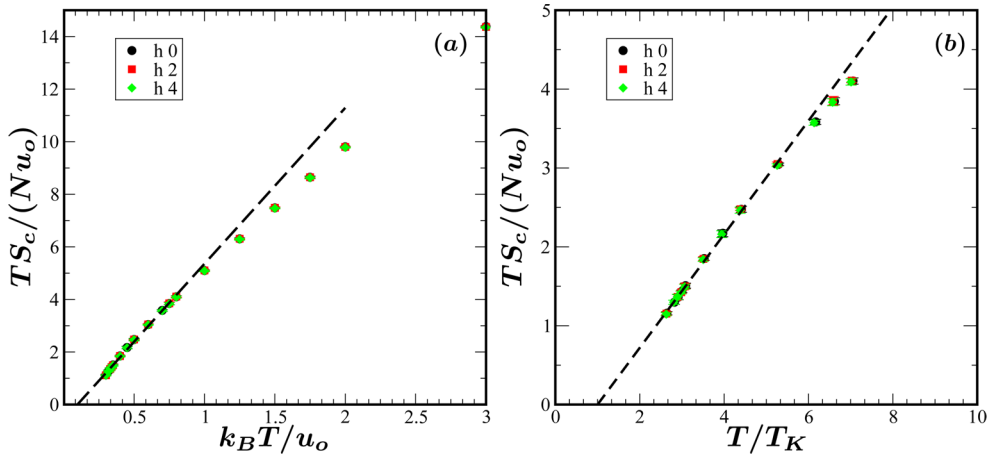

Figure 10. Thermodynamic fragility of the system is independent of the barrier height. (a) Temperature dependence of TS_c for the model to determine the Kauzmann temperature. The line represents the linear fit using $TS_c = K_T(T/T_K - 1)$. (b) The scaled plot with $T_K = 0.11$ shows that the thermodynamic fragility $K_T = 0.72$ is the same for all barrier heights.

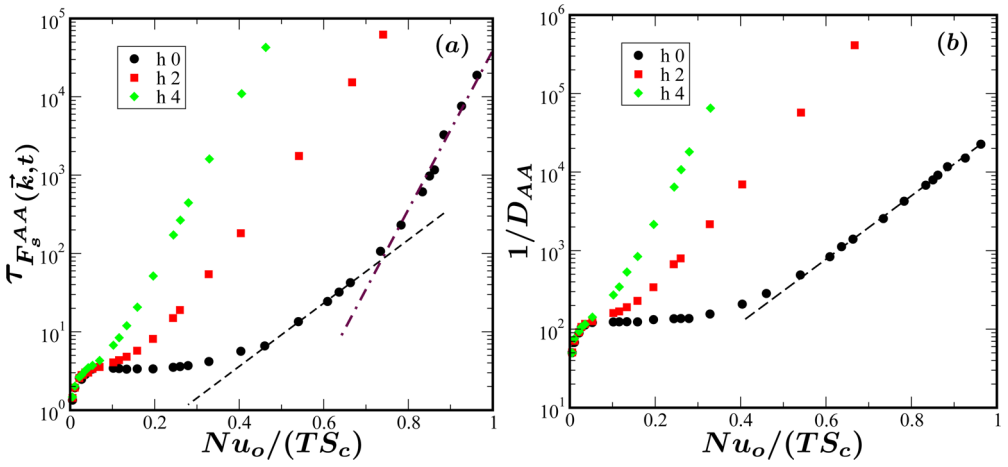

Figure 11. Adam–Gibbs plot for (a) relaxation times and (b) diffusion coefficients, for different choices of barrier height. The Adam–Gibbs relation does not seem to hold for $h = 0$ very well in either case, though it is better observed for diffusion coefficients. For low temperatures and for finite h values, the agreement with the Adam–Gibbs relation is better. The fit lines for $h = 0$ are used to obtain the Adam–Gibbs coefficient A_D, which is used in the plot of relaxation times (dashed line). On the basis of the fractional Stokes–Einstein behavior observed in Figure 14, the dash-dotted line using A_D/ζ instead of A_D describes the expected behavior of relaxation times at low temperatures, and is found to describe the simulation data very well.

where $A(h) = A(0) + hS_c/k_B$. This quantity is of course not temperature independent, but we choose the value of S_c at a high temperature of $T = 0.8$ (where S_c is maximum) to obtain values for $A(h)$, which are used in Figure 13 to plot relaxation times and

DOI: 10.1021/acs.jpcb.5b03122
J. Phys. Chem. B 2015, 119, 11243–11252

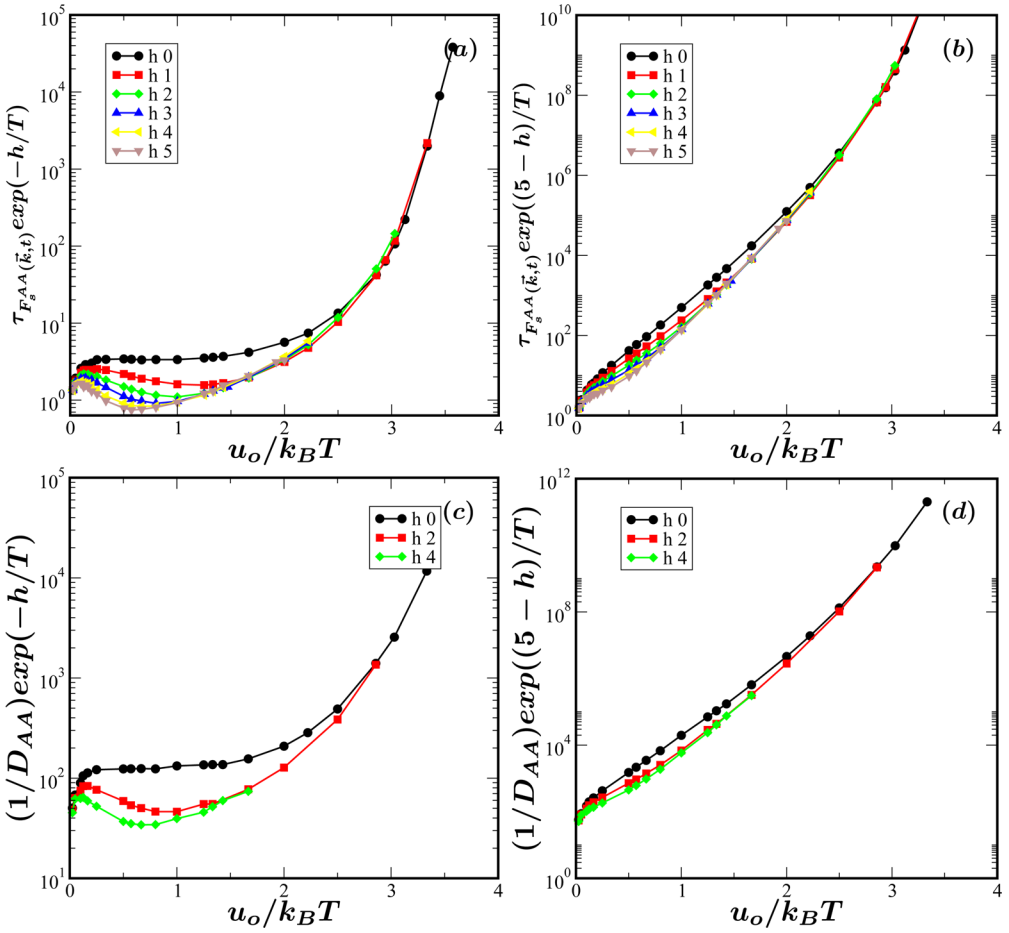

Figure 12. Relaxation times multiplied by (a) $\exp(-h/k_BT)$ and (b) $\exp(5 - h/k_BT)$ to scale out the change of bond lifetime. In both cases, the τ values overlap at low temperatures, indicating that the "intrinsic" dependence of relaxation times on temperature is not affected by the barrier heights. The superposition of data is not good (worse in part a) at high temperatures, where anomalous behavior of dynamics is observed. The corresponding plots for the diffusion coefficient are shown in parts c and d.

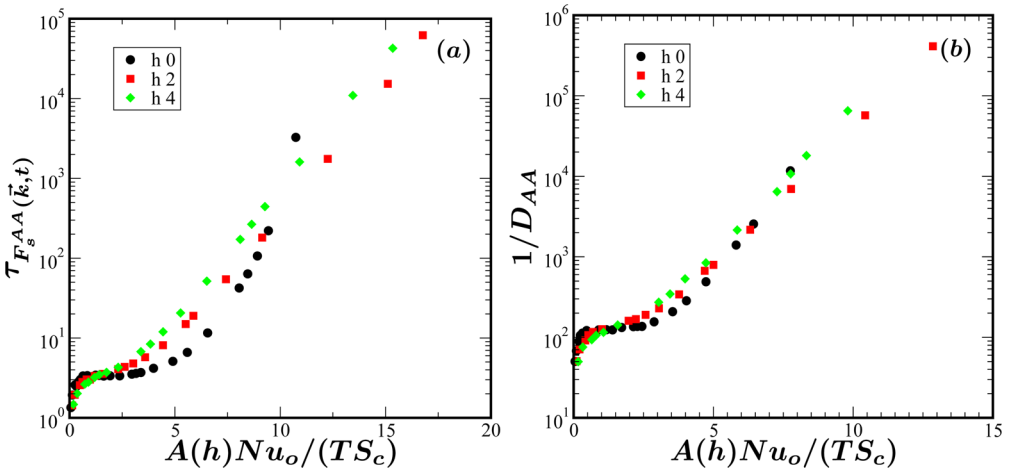

Figure 13. Adam–Gibbs plot with estimated $A(h)$ for (a) relaxation time and (b) diffusion coefficient. While the scaling does not produce a very good data collapse for relaxation times, the collapse is reasonable for the diffusion coefficient, with the observation of a low temperature region where the Adam–Gibbs relation is obeyed.

diffusion coefficients against $A(h)/TS_c$. We find that the relaxation times do not scale so well, but the diffusion coefficients show a satisfactory data collapse.

We now return to the observation earlier that the Adam–Gibbs relation is reasonably well observed for diffusion coefficients for $h = 0$, whereas they are not in the case of relaxation times. In the original formulation, the Adam–Gibbs relation was derived for particle mobilities, and thus *a priori* applicable to diffusion, and only by association to relaxation times. However, in view of the known breakdown of the Stokes–

DOI: 10.1021/acs.jpcb.5b03122
J. Phys. Chem. B 2015, 119, 11243–11252

Einstein relationship, the Adam−Gibbs relation cannot be valid both for diffusion and relaxation times. This situation has not been directly addressed previously, to our knowledge, since most studies have focused on a temperature regime where a *fractional* Stokes−Einstein result appears valid. In our study, we straddle the temperature window where both the Stokes−Einstein and fractional Stokes−Einstein relations are valid. We show, in Figure 14, a Stokes−Einstein plot, which demonstrates that, for $h = 0$,

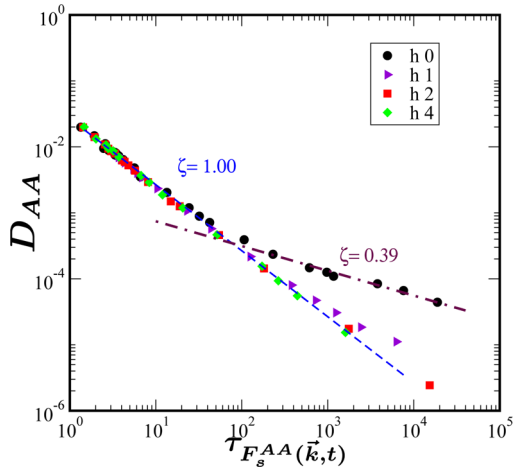

Figure 14. Stokes−Einstein plot showing diffusion coefficients plotted against relaxation times. For $h = 0$, the data shows that the Stokes−Einstein relation is strongly violated at low temperatures, with a fractional Stokes−Einstein exponent of $\zeta = 0.39$.

the Stokes−Einstein relation is strongly violated at low temperatures. Representing by A_D the Adam−Gibbs free energy for diffusion, the corresponding free energy for relaxation times may be written as $A_\tau = -A_D/\zeta$, where $\zeta = 1$ when the Stokes−Einstein relation holds. The slopes (on a semilog plot) A_τ for the two regimes, shown in Figure 11 for relaxation times, convincingly demonstrate that the apparent deviation from Adam−Gibbs behavior of the relaxation times is indeed extremely well explained by the known violation of the Stokes−Einstein relation, along with the expectation that the Adam−Gibbs relation holds principally for diffusion coefficients rather than relaxation times. To our knowledge, this is the first time that the validity of the Adam−Gibbs relation for diffusion coefficients vs relaxation times has been explored to show convincingly that the AG relation is valid primarily for diffusion coefficients rather than other related quantities such as relaxation times.

DISCUSSION AND CONCLUSIONS

A principal conclusion that is apparent from the work described is that changes in the details of interactions between particles that do not affect their thermodynamics can have a strong influence on the dynamics, in a sufficiently nontrivial manner that one may deduce from the analysis of dynamical data dramatically different characterizations, such as widely different fragilities. To a first approximation, we can view the dynamics of the studied system for different barriers as being simply related, and therefore that their intrinsic fragilities are the same. Such a view would privilege in the present case the thermodynamic fragility as the "true" fragility, and lead one to argue that the apparent differences in measured kinetic fragilities arise from the additional contribution of the changes in high temperature activation energy. Such a view, however, is not consistent with treating the dynamical data as the primary object of classification according to fragility, nor with analyses that have argued that high temperature activation energy scales should be factored out in order for fragility to be evaluated properly. Our results therefore highlight an ambiguity in the definition of fragilty that needs to be sorted out by future work.

Our work should also be treated as preliminary for other reasons. The first is the choice of the model system. For the given choice of parameters, the presence of a diffusion anomaly proves to be an inconvenience, and other parametrizations need to be considered to avoid this situation. The second reason is the observation that the Adam−Gibbs relation appears to not be so well observed in this system. The possible origins are the definition of basins which are specific to this class of models with discrete interaction energies, and the possibility that the violation of the Stokes−Einstein relation in this system means that the Adam−Gibbs relation is not simultaneously valid for both diffusion coefficients and relaxation times. Both of these are interesting questions in their own right. Our results concerning the violation of the Stokes−Einstein relation, however, convincingly show that the Adam−Gibbs relation is valid at low temperatures for diffusion coefficients, and the observed lack of conformity in the case of the relaxation times stems directly from the violation of the Stokes−Einstein relation. Finally, the question of how best to quantify fragility remains open at the end of the present exercise and must be pursued further to a satisfactory resolution. Further work is in progress to address these issues.

AUTHOR INFORMATION

Corresponding Author

*Phone: +91-80-22082838. Fax: +91-80-22082767. E-mail: sastry@jncasr.ac.in.

Notes

The authors declare no competing financial interest.

ACKNOWLEDGMENTS

We acknowledge the support of the TUE-CMS, JNCASR, and the SSL, JNCASR, for computational resources. We acknowledge discussions with C. A. Angell, G. Tarjus, J. Dyre, J. F. Douglas, and Biman Bagchi on various aspects of work related to the analysis of fragility.

REFERENCES

(1) Angell, C. A. Relaxation in liquids, polymers and plastic crystals-strong/fragile patterns and problems. *J. Non-Cryst. Solids* **1991**, *131*, 13−31.

(2) Greer, A. L.; Kelton, K. F.; Sastry, S. *Fragility in Glass-Forming Liquids*; Hindustan Book Agency: Gurgaon, India, 2014.

(3) Adam, G.; Gibbs, J. H. On the temperature dependence of cooperative relaxation properties in glass-forming liquids. *J. Chem. Phys.* **1965**, *43*, 139−146.

(4) Martinez, L. M.; Angell, C. A. A thermodynamic connection to the fragility of glass-forming liquids. *Nature* **2001**, *410*, 663−667.

(5) Goldstein, M. Viscous liquids and the glass transition. V. Sources of the excess specific heat of the liquid. *J. Chem. Phys.* **1976**, *64*, 4767−4774.

(6) Stillinger, F. H.; Weber, T. A. Hidden structure in liquids. *Phys. Rev. A: At., Mol., Opt. Phys.* **1982**, *25*, 978−989.

(7) Sciortino, F.; Kob, W.; Tartaglia, P. Inherent Structure Entropy of Supercooled Liquids. *Phys. Rev. Lett.* **1999**, *83*, 3214−3217.

DOI: 10.1021/acs.jpcb.5b03122
J. Phys. Chem. B 2015, 119, 11243−11252

(8) Sastry, S. The relationship between fragility, configurational entropy and the potential energy landscape of glass-forming liquids. *Nature (London, U. K.)* **2001**, *409*, 164−167.
(9) Sciortino, F. Potential energy landscape description of supercooled liquids and glasses. *J. Stat. Mech.: Theory Exp.* **2005**, *2005*, P05015.
(10) Heuer, A. Exploring the potential energy landscape of glass-forming systems: from inherent structures via metabasins to macroscopic transport. *J. Phys.: Condens. Matter* **2008**, *20*, 373101−373155.
(11) Abraham, S. E.; Bhattacharrya, S. M.; Bagchi, B. Energy Landscape, Antiplasticization, and Polydispersity Induced Crossover of Heterogeneity in Supercooled Polydisperse Liquids. *Phys. Rev. Lett.* **2008**, *100*, 167801.
(12) Dudowicz, J.; Freed, K. F.; Douglas, J. F. Fragility of glass-forming polymer liquids. *J. Phys. Chem. B* **2005**, *109*, 21350−21356.
(13) Dudowicz, J.; Freed, K. F.; Douglas, J. F. Direct computation of characteristic temperatures and relaxation times for glass-forming polymer liquids. *J. Chem. Phys.* **2005**, *123*, 111102.
(14) Mattsson, J.; Wyss, H. M.; Fernandez-Nieves, A.; Miyazaki, K.; Hu, Z.; Reichman, D. R.; Weitz, D. A. Soft colloids make strong glasses. *Nature* **2009**, *462*, 83−86.
(15) Bordat, P.; Affouard, F.; Descamps, M.; Ngai, K. L. Does the Interaction Potential Determine Both the Fragility of a Liquid and the Vibrational Properties of Its Glassy State? *Phys. Rev. Lett.* **2004**, *93*, 105502.
(16) Bordat, P.; Affouard, F.; Descamps, M. Effect of anharmonicity on the diffusion in glassforming binary Lennard-Jones systems. *J. Non-Cryst. Solids* **2007**, *353*, 3924−3927.
(17) Sengupta, S.; Vasconcelos, F.; Affouard, F.; Sastry, S. Dependence of the fragility of a glass former on the softness of interparticle interactions. *J. Chem. Phys.* **2011**, *135*, 194503.
(18) Ruocco, G.; Sciortino, F.; Zamponi, F.; De Michele, C.; Scopigno, T. Landscapes and Fragilities. *J. Chem. Phys.* **2004**, *120*, 10666−10680.
(19) Alba-Simionesco, C.; Kivelson, D.; Tarjus, G. Temperature, density, and pressure dependence of relaxation times in supercooled liquids. *J. Chem. Phys.* **2002**, *116*, 5033−5038.
(20) Tarjus, G.; Kivelson, D.; Mossa, S.; Alba-Simionesco, C. Disentangling density and temperature effects in the viscous slowing down of glassforming liquids. *J. Chem. Phys.* **2004**, *120*, 6135−6141.
(21) Gnan, N.; Schrøder, T. B.; Pedersen, U. R.; Bailey, N. P.; Dyre, J. C. Pressure-energy correlations in liquids. IV. "Isomorphs" in liquid phase diagrams. *J. Chem. Phys.* **2009**, *131*, 234504.
(22) Sengupta, S.; Schrøder, T. B.; Sastry, S. Density-temperature scaling of the fragility in a model glass-former. *Eur. Phys. J. E: Soft Matter Biol. Phys.* **2013**, *36*, 141.
(23) Angell, C. A. In *Hydrogen Bonded Liquids*; Dore, J. C., Teixeira, J., Eds.; NATO ASI E; Kluwer Academic Publishers: Dordrecht, The Netherlands, 1991; Vol. *329*, pp 59−79.
(24) Saika-Voivod, I.; Zaccarelli, E.; Sciortino, F.; Buldyrev, S. V.; Tartaglia, P. Effect of bond lifetime on the dynamics of a short-range attractive colloidal system. *Phys. Rev. E: Stat. Phys., Plasmas, Fluids, Relat. Interdiscip. Top.* **2004**, *70*, 041401.
(25) Zaccarelli, E.; Foffi, G.; Dawson, K. A.; Buldyrev, S. V.; Sciortino, F.; Tartaglia, P. Confirmation of anomalous dynamical arrest in attractive colloids: A molecular dynamics study. *Phys. Rev. E: Stat. Phys., Plasmas, Fluids, Relat. Interdiscip. Top.* **2002**, *66*, 041402.
(26) Foffi, G.; Angelani, L. Short range attractive colloids: dynamics and energy landscape properties. *J. Phys.: Condens. Matter* **2008**, *20*, 075108.
(27) Alder, B. J.; Wainwright, T. E. Studies in molecular dynamics. I. General method. *J. Chem. Phys.* **1959**, *31*, 459−466.
(28) Lowe, C. P. An alternative approach to dissipative particle dynamics. *Europhys. Lett.* **1999**, *47*, 145.
(29) Nikunen, P.; Karttunen, M.; Vattulainen, I. How would you integrate the equations of motion in dissipative particle dynamics simulations? *Comput. Phys. Commun.* **2003**, *153*, 407−423.
(30) Sastry, S. Liquid limits: Glass transition and liquid-gas spinodal boundaries of metastable liquids. *Phys. Rev. Lett.* **2000**, *85*, 590.
(31) Frenkel, D.; Ladd, A. J. New Monte Carlo method to compute the free energy of arbitrary solids. Application to the fcc and hcp phases of hard spheres. *J. Chem. Phys.* **1984**, *81*, 3188−3193.
(32) Frenkel, D.; Smit, B. *Understanding molecular simulation: from algorithms to applications*; Academic Press: San Diego, CA, USA, 2002.
(33) Allen, M. P.; Tildesley, D. J. *Computer Simulation Of Liquids*; Oxford University Press: Oxford, UK, 1987.
(34) Moreno, A. J.; Buldyrev, S. V.; La Nave, E.; Saika-Voivod, I.; Sciortino, F.; Tartaglia, P.; Zaccarelli, E. Energy Landscape of a Simple Model for Strong Liquids. *Phys. Rev. Lett.* **2005**, *95*, 157802.

DOI: 10.1021/acs.jpcb.5b03122
J. Phys. Chem. B 2015, 119, 11243−11252